arXiv:1006.3855v1 [cs.IT] 19 Jun 2010

# Impact of Channel Asymmetry on Performance of Channel Estimation and Precoding for Downlink Base Station Cooperative Transmission

Xueying Hou, *Student Member, IEEE*, Chenyang Yang, *Senior Member, IEEE*,
and Buon Kiong (Vincent) Lau, *Senior Member, IEEE*

## Abstract

Base station (BS) cooperative transmission can improve the spectrum efficiency of cellular systems, whereas using which the channels will become *asymmetry*. In this paper, we study the impact of the *asymmetry* on the performance of channel estimation and precoding in downlink BS cooperative multiple-antenna multiple-carrier systems. We first present three linear estimators which jointly estimate the channel coefficients from users in different cells with minimum mean square error, robust design and least square criterion, and then study the impact of *uplink channel asymmetry* on their performance. It is shown that when the large scale channel information is exploited for channel estimation, using non-orthogonal training sequences among users in different cells leads to minor performance loss. Next, we analyze the impact of *downlink channel asymmetry* on the performance of precoding with channel estimation errors. Our analysis shows that although the estimation errors of weak cross links are large, the resulting rate loss is minor because their contributions are weighted by the receive SNRs. The simulation results verify our analysis and show that the rate loss per user is almost constant no matter where the user is located, when the channel estimators exploiting the large scale fading gains.

## Index Terms

Base station cooperative transmission, channel estimation, channel asymmetry.

X. Hou and C. Yang are with the School of Electronics and Information Engineering, Beihang University (BUAA), Beijing, 100191, China (e-mail: hxymr@ee.buaa.edu.cn; cyyang@buaa.edu.cn). B. K. Lau is with the Department of Electrical and Information Technology, Lund University, SE-221 00 Lund, Sweden (e-mail: bkl@eit.lth.se).

# I. INTRODUCTION

Base station (BS) cooperative transmission, which is also known as coordinated multi-point transmission (CoMP), is an effective way to mitigate the inter-cell interference (ICI) arisen from universal frequency reuse cellular systems. As a promising transmit strategy, coherent cooperative transmission can enhance the downlink spectrum efficiency by using multiuser (MU) multiple-input multiple-output (MIMO) precoding [1, 2], when both data and channel state information (CSI) are gathered at a central unit (CU) via backhaul links.

In non-cooperative systems, each BS only needs to estimate the CSI of *local channels, i.e.,* the channels between the BS and the mobile stations (MSs) that are in the same cell. If the training sequences for the MSs in different cells are not orthogonal, the channel estimation performance will severely degrade due to the ICI [3–7]. The impact of the ICI can be mitigated by designing training sequences with low cross-correlation for the MSs in different cells [4], or by developing channel estimators exploiting the interference statistics [5]. In [6], the authors propose to use non-uniform pilot density and a DFT-based channel estimator to first separate and then subtract the interference signal from the estimated channel impulse response (CIR). Assuming that the desired channels and the interfered channels do not overlap and their interference-free initial estimates can be obtained through orthogonal training, the authors in [7] propose to exploit the delay subspace structure to improve the estimation performance of the desired channels.

In coherent cooperative transmission systems, the CSI of *cross channels,* i.e., the channels between the BSs and the MSs who are in different cells, needs to be estimated as well. Both the local and cross channel coefficients can be jointly estimated using the conventional estimators such as those in [8] when the training signals are orthogonal both for the MSs within a cell and for the MSs among the coordinated cells. However, large overhead is inevitable if orthogonal training signals are used for all MSs in the cooperative cell cluster. Moreover, this demands inter-cell signalling and protocol to coordinate the training sequences [9]. Such a burden will become more noticeable when the cooperative clusters are formed in a dynamic way [10]. In [11], the authors suggest to spread the orthogonal sequences from slot to slot, which may lead to outdated CSI at the transmitter under time-varying channels. Considering the propagation delay differences in multicell channels, a group of orthogonal training sequences that are robust to the delay are designed in [12], but the number of sequences in the group is limited.

An inherent feature of the channels in CoMP systems is *asymmetry*. On one hand, the multi-cell downlink channels are *asymmetric*, which means that the average channel gains from different BSs to one MS are different. On the other hand, the multi-cell uplink channels are also *asymmetric*, which means that the average channel gains from MSs in different cells to one BS differ. Such an asymmetric channel feature is fundamental in CoMP systems, since the difference of the large scale fading gains cannot be compensated by an uplink or downlink power control mechanism. Specifically, if the MSs in different cells compensate their large scale fading gain differences towards one BS by power control, their receive signal energy differences towards other BSs will increase. This is analogous to the interference asynchrony feature, which cannot be dealt with by time-advanced techniques [13].

In this paper, we study the impact of the channel *asymmetry* on the performance of joint channel estimators and on the performance of downlink BS cooperative MIMO orthogonal frequency-division multiplexing (OFDM) systems with channel estimation errors.

Firstly, we introduce three joint estimators requiring different channel statistics, which are the minimum mean square error (MMSE) estimator, a robust estimator and the least square (LS) estimator. We analyze the performance of these estimators when the *uplink channel asymmetry* is exploited. Our analysis shows that if the training sequences are not orthogonal among cells, the LS estimator will perform significantly worse than using orthogonal sequences. On the other hand, the MMSE and robust estimators have minor performance loss from those using orthogonal sequences, thanks to the large attenuation of the cross channels.

Secondly, we analyze the impact of channel estimation errors on the performance of CoMP[1] system using zero forcing beamforming (ZFBF) by deriving the rate loss led by the channel estimation errors. At the first glance, the cross channels that experience large path loss are hard to estimate in practice since the transmission power at the MS side is limited [2,14], which may degrade the downlink transmission performance. Nonetheless, our analysis shows that when the training sequences are orthogonal and the joint MMSE estimator is applied, the contribution of channel estimation errors to the rate loss is weighted by the receive SNR of the corresponding channel link. As a result, even though the channel estimation errors of cross channels are large, their impact on the rate loss is minor owing to the fact that the receive SNRs of the cross links are considerably lower than the local link. Interestingly, simulation results demonstrate that the rate loss of MS is nearly invariant no matter if the MS is located at the cell edge or cell center.

---

[1] There are various transmission strategies for CoMP transmission such as coherent and non-coherent transmission. For simplicity, we refer the coherent BS cooperative transmission using MU MIMO precoding as CoMP transmission in the following.

The rest of the paper is organized as follows. Section II introduces the system and channel models. Section III and IV respectively present three joint channel estimators and analyze their performance. In Section V, we analyze the impact of channel estimation errors on downlink CoMP transmission. Simulation results are provided in Section VI to verify our analysis and to evaluate the system performance. The paper is concluded in Section VII.

*Notations:* Boldface upper and lower case letters $\mathbf{X}$ and $\mathbf{x}$ represent matrices and vectors, and standard lower case letters $x$ denote scalars. $\mathbf{X}^T$, $\mathbf{X}^H$ and $tr\{\mathbf{X}\}$ denote the transpose, Hermitian conjugate transpose and the trace of $\mathbf{X}$. $\mathbf{X}(i,i)$, $\mathbf{X}(i,:)$ and $\mathbf{X}(:,i)$ represent the $(i,i)$th element, the $i$th row and the $i$th column of $\mathbf{X}$, respectively. $\|\mathbf{x}\|$ represents the two-norm of $\mathbf{x}$, and $\mathrm{diag}\{\mathbf{x}\}$ is a diagonal matrix with its elements. $\mathbb{E}\{x\}$ is the expectation of a random variable $x$. $\Re\{x\}$ and $|x|$ stand for the real part and the norm of a complex scalar $x$. $\lfloor x \rfloor$ denotes the largest integer no larger than a real number $x$ and $\lceil x \rceil$ represents the smallest integer no smaller than $x$. Finally, $\mathbf{I}_N$ denotes the identity matrix of size $N$, and $\mathbf{0}$ denotes the matrix of zeros.

## II. SYSTEM AND CHANNEL MODELS

### A. BS Cooperative Transmission System and Channel Models

Consider a centralized CoMP system, where $B$ BSs each equipped with $N_t$ antennas cooperatively serve $M$ single-antenna MSs. We consider time division duplexing (TDD) systems, where the CSI required for MU MIMO precoding is obtained through uplink training by exploiting the channel reciprocity. In the uplink training phase, all MSs send training sequences and each BS estimates the CSI from all MSs to it. Then the BSs forward the estimated CSI to the CU via low latency backhaul links. The CU computes the precoding and then sends back the precoding vectors to each BS for downlink transmission.

We consider frequency selective channels. The channel is assumed to be quasi-static, which means that the channel remains constant during the uplink training and the downlink transmission. The composite CIR from MS $m$ to antenna $a$ of BS $b$ can be expressed as $\mathbf{g}^t_{m,b,a} = \alpha_{m,b}\mathbf{h}^t_{m,b,a}$, where $\mathbf{g}^t_{m,b,a} = [g^t_{m,b,a}(0), \cdots, g^t_{m,b,a}(L-1)]^T \in \mathbb{C}^{L\times 1}$, $\alpha_{m,b}$ is the large scale fading coefficient including path loss and shadowing, $\mathbf{h}^t_{m,b,a} = [h^t_{m,b,a}(0), \cdots, h^t_{m,b,a}(L-1)]^T \in \mathbb{C}^{L\times 1}$ is the small scale fading channel vector, $h^t_{m,b,a}(l)$ is the fading coefficient of the $l$th resolvable path, which is a complex Gaussian random variable with zero mean and variance $\sigma_{h_l}^2$, and $L$ is the number of resolvable paths. We assume that $\sum_{l=0}^{L-1}\sigma_{h_l}^2 = 1$.

### B. Uplink Training Phase

Except that the uplink channels are asymmetric, the signal received at one BS from MSs in different cells are asynchronous in CoMP systems [13]. Denote the propagation delay from MS $m$ to BS $b$ as $\tau_{m,b}$. We assume that the cyclic prefix in the OFDM symbol is long enough, such that the propagation delays turn into phase shifts in the frequency domain channels.

Consider that all $M$ MSs in the cooperative cluster send training sequences during the same uplink training duration. Denote the frequency domain training sequence of the $m$th MS as $\mathbf{t}_m = [t_m(0), \cdots, t_m(K-1)]^T \in \mathbb{C}^{K\times 1}$, its transmit power at each subcarrier as $p_m^u$, then the received signal of the $k$th subcarrier at antenna $a$ of BS $b$ can be expressed as

$$r_{b,a}(k) = \sum_{m=1}^{M} \sqrt{p_m^u}\, t_m(k) g_{m,b,a}^f(k) + n(k), \tag{1}$$

where $g_{m,b,a}^f(k) = \sum_{l=0}^{L-1}\alpha_{m,b} h_{m,b,a}^t(l - \frac{\tau_{m,b}}{T_s})\exp(-j\frac{2\pi}{K}lk)$ denotes the composite channel frequency response (CFR) at the $k$th subcarrier including both large scale fading and phase shift led by propagation delay, $T_s$ is the sampling period, $K$ is the subcarriers number of OFDM system, $h_{m,b,a}^f(k) = \sum_{l=0}^{L-1} h_{m,b,a}^t(l)\exp(-j\frac{2\pi}{K}lk)$ represents the small scale CFR at the $k$th subcarrier, $n(k)$ is the additive white Gaussian noise (AWGN) with zero mean and variance $\sigma_n^2$.

With the received signal, BS $b$ estimates the composite CFR between its multiple antennas and all MSs, $\hat{\mathbf{G}}_b^f(k) = [\hat{\mathbf{g}}_{1,b}^f(k), \cdots, \hat{\mathbf{g}}_{M,b}^f(k)]^H \in \mathbb{C}^{M\times N_t}$, where $\hat{\mathbf{g}}_{m,b}^f(k) = [\hat{g}_{m,b,1}^f(k), \cdots, \hat{g}_{m,b,N_t}^f(k)]^T$ is the CFR estimate between MS $m$ and the multiple antennas of BS $b$. Then the BS forwards $\hat{\mathbf{G}}_b^f(k)$ to the CU, as illustrated in Fig. 1 for a two-cell CoMP system.

### C. Downlink Transmission Phase

The CU collects the estimated composite CFR from each BS via a low latency backhaul, and integrates the estimated global channel as $\hat{\mathbf{G}}^f(k) = [\hat{\mathbf{G}}_1^f(k), \cdots, \hat{\mathbf{G}}_B^f(k)] \in \mathbb{C}^{M\times BN_t}$. Then, the CU computes the multi-cell precoding $\mathbf{V}(k)$ based on $\hat{\mathbf{G}}^f(k)$, and sends the downlink data and the corresponding precoder to each BS, as illustrated in Fig. 2.

The downlink composite channels from multiple BSs to MS $m$ can be expressed as $\mathbf{g}_m^f(k) = [(\mathbf{g}_{m,1}^f(k))^H, \cdots, (\mathbf{g}_{m,B}^f(k))^H]^H$, where $\mathbf{g}_{m,b}^f(k) \in \mathbb{C}^{N_t\times 1}$ is the channel vector between all antennas of BS $b$ and MS $m$. Let $d_m(k)$ be the data intended for MS $m$ at the $k$th subcarrier. For simplicity and without loss of generality, we assume that $\mathbb{E}\{d_m^*(k)d_m(k)\} = 1$. Denote $\mathbf{v}_m(k) \in \mathbb{C}^{BN_t \times 1}$ as the precoding vector for MS $m$ under CoMP transmission, and $p_m^d(k)$ as the power allocated to MS $m$ at the $k$th subcarrier. Then the receive signal at MS $m$ is

$$y_m(k) = \sqrt{p_m^d(k)}(\mathbf{g}_m^f(k))^H \mathbf{v}_m(k) d_m(k) + \sum_{j=1, j\neq m}^{M} \sqrt{p_j^d(k)}(\mathbf{g}_m^f(k))^H \mathbf{v}_j(k) d_j(k) + z_m(k), \quad (2)$$

where $z_m(k)$ is the AWGN with zero mean and variance $\sigma_z^2$ experienced at MS $m$.

## III. UPLINK CHANNEL ESTIMATION FOR DOWNLINK COMP TRANSMISSION

As shown in the downlink transmission model, the composite CFR is required for precoding in CoMP OFDM systems, rather than the small scale fading CFR.

The performance of channel estimation for the composite CFR depends both on the channel features and on the information known *a priori*. In this paper, we assume that the propagation delays and the number of resolvable paths can be estimated perfectly. In practice, they can be estimated using various techniques such as those shown in [7,15]. Since the number of resolvable paths is usually much less than the number of subcarriers in practical systems, the performance of channel estimation can be significantly improved by exploiting the frequency correlation of the channels [8]. When the propagation delays and the number of resolvable paths are known, this can simply be implemented by first estimating the composite CIR, and then obtaining the CFR by Fourier transformation. In the following, we only address the CIR estimation.

To simplify our analysis, we assume that the transmit power for each MS's training sequence is equal. The frequency domain receive signal in (1) can be rewritten as a more compact form

$$\begin{aligned} \mathbf{r}_{b,a} &= \sqrt{p^u} \sum_{m=1}^{M} \mathbf{T}_m \mathbf{g}_{m,b,a}^f + \mathbf{n} = \sqrt{p^u} \sum_{m=1}^{M} \mathbf{T}_m \mathbf{\Phi}_{m,b} \alpha_{m,b} \mathbf{F} \mathbf{h}_{m,b,a}^t + \mathbf{n} \\ &= \sqrt{p^u} \sum_{m=1}^{M} \mathbf{X}_{m,b} \mathbf{g}_{m,b,a}^t + \mathbf{n} = \sqrt{p^u} \mathbf{X} \mathbf{g}_{b,a}^t + \mathbf{n}, \end{aligned} \quad (3)$$

where $\mathbf{r}_{b,a} = [r_{b,a}(0), \cdots, r_{b,a}(K-1)]^T$, $\mathbf{T}_m = \mathrm{diag}\{\mathbf{t}_m\}$, $\mathbf{g}_{m,b,a}^f = [g_{m,b,a}^f(0), \cdots, g_{m,b,a}^f(K-1)]^T$ denotes the composite CFR vector from MS $m$ to the $a$th antenna of BS $b$, $\mathbf{\Phi}_{m,b} = \mathrm{diag}\{[\psi_{m,b}(0), \cdots, \psi_{m,b}(K-1)]\}$, $\psi_{m,b}(k) = \exp(-j\frac{2\pi}{K}\frac{\tau_{m,b}}{T_s}k)$, $\mathbf{F} \in \mathbb{C}^{K\times L}$ is the first $L$ columns of a $K \times K$ Fourier transform matrix, $\mathbf{X}_{m,b} = \mathbf{T}_m \mathbf{\Phi}_{m,b} \mathbf{F} \in \mathbb{C}^{K\times L}$ is the equivalent training matrix of MS $m$ by considering the known $\tau_{m,b}$ and $L$, $\mathbf{X} = [\mathbf{X}_{1,b}, \cdots, \mathbf{X}_{M,b}] \in \mathbb{C}^{K\times ML}$ is an equivalent training matrix of all MSs, $\mathbf{g}^t_{b,a} = [(\mathbf{g}^t_{1,b,a})^T, \cdots, (\mathbf{g}^t_{M,b,a})^T]^T \in \mathbb{C}^{ML\times 1}$ is the composite CIR vector from all MSs to antenna $a$ of BS $b$. $\mathbf{n}$ is the AWGN vector with zero mean and covariance matrix $\sigma_n^2\mathbf{I}_K$.

Since each BS needs to estimate both local and cross channels for CoMP transmission, it is natural to estimate the CIRs from all MSs jointly, i.e., to estimate $\mathbf{g}^t_{b,a}$. Denote the estimation errors of $\mathbf{g}^t_{b,a}$ as $\tilde{\mathbf{g}}^t_{b,a} = \mathbf{g}^t_{b,a} - \hat{\mathbf{g}}^t_{b,a}$, and its MSE as $\mathrm{MSE}_{b,a} = \mathbb{E}\{\|\tilde{\mathbf{g}}^t_{b,a}\|^2\} = \mathbb{E}\{\sum_{m=1}^M \|\tilde{\mathbf{g}}^t_{m,b,a}\|^2\}$. The MMSE estimator can be readily derived from (3) by minimizing the $\mathrm{MSE}_{b,a}$, which yields,

$$\hat{\mathbf{g}}^{t^{\mathrm{MMSE}}}_{b,a} = \left(\mathbf{X}^H\mathbf{X} + \frac{\sigma_n^2}{p^u}\mathbf{R}^{-1}_{b,a}\right)^{-1}\mathbf{X}^H\mathbf{r}_{b,a}, \tag{4}$$

where $\mathbf{R}_{b,a} = \mathbb{E}\{\mathbf{g}_{b,a}\mathbf{g}^H_{b,a}\}$ is the covariance matrix of the channels from all $M$ MSs to the $a$th antenna of BS $b$. Assume that the small scale fading channels among different BS-MS links are uncorrelated. Then $\mathbf{R}_{b,a} = \mathrm{diag}\{[\alpha^2_{1,b}\mathbf{R}_{1,b,a}, \ldots, \alpha^2_{M,b}\mathbf{R}_{M,b,a}]\}$, $\mathbf{R}_{m,b,a}$ is the covariance matrix of the small scale fading channel vector from MS $m$ to the $a$th antenna of BS $b$.

Although both $\mathbf{R}_{m,b,a}$ and $\alpha^2_{m,b}$ vary slowly and can be estimated in practice [16], $\alpha^2_{m,b}$ is a scalar parameter that can be estimated more accurately and requires a much lower feedback rate. When $\alpha^2_{m,b}$ is estimated perfectly but $\mathbf{R}_{m,b,a}$ is unknown, by assuming uniform power delay profile (PDP) for small scale fading channels similarly to the conventional robust channel estimation algorithms [17], we obtain a robust channel estimator,

$$\hat{\mathbf{g}}^{t^{\mathrm{robust}}}_{b,a} = \left(\mathbf{X}^H\mathbf{X} + \frac{\sigma_n^2}{p^u}\mathbf{D}^{-1}_{b,a}\right)^{-1}\mathbf{X}^H\mathbf{r}_{b,a}, \tag{5}$$

where $\mathbf{D}_{b,a} = \mathrm{diag}\{[\alpha^2_{1,b}\frac{1}{L}\mathbf{I}_L, \ldots, \alpha^2_{M,b}\frac{1}{L}\mathbf{I}_L]\}$.

When we know nothing more than $\tau_{m,b}$ and $L$, we can apply the LS estimator as

$$\hat{\mathbf{g}}^{t^{\mathrm{LS}}}_{b,a} = \left(\mathbf{X}^H\mathbf{X}\right)^{-1}\mathbf{X}^H\mathbf{r}_{b,a}. \tag{6}$$

## IV. PERFORMANCE ANALYSIS OF THE CHANNEL ESTIMATORS

In this section, we analyze the performance of the joint channel estimators. We derive the MSE of the composite CIR estimates. Then we discuss the impact on the performance of the estimators when the training sequences are *orthogonal* or *non-orthogonal*.

When more than two MSs send training sequences in the uplink, it is nontrivial to obtain an explicit expression of the MSE of the CIR estimate. For mathematical tractability, we consider a simple but fundamental scenario, where $B$ multiple-antenna BSs cooperatively serve two single-antenna MSs, i.e., $M = 2$, and the two MSs are located in two cells.

### *A. MSE of Three Estimators*

We first derive the estimation error covariance matrix of the CIRs from all MSs to the $a$th antenna of the $b$th BS, $\mathbf{R}_{\tilde{\mathbf{g}}_{b,a}} = \mathbb{E}\{\tilde{\mathbf{g}}_{b,a}^t(\tilde{\mathbf{g}}_{b,a}^t)^H\}$, and then we can get the MSE of the CIR estimation as $\mathrm{MSE}_{m,b,a} = \sum_{i=(m-1)L+1}^{mL} \mathbf{R}_{\tilde{\mathbf{g}}_{b,a}^t}(i,i)$. From (4), (5) and (6), the covariance matrix for the estimators can be obtained as follows by applying the Woodbury matrix identity [18],

$$\mathbf{R}_{\tilde{\mathbf{g}}_{b,a}^t}^{\mathrm{MMSE}} = \left(\mathbf{R}_{b,a}^{-1} + \frac{p^u}{\sigma_n^2}\mathbf{B}\right)^{-1}, \tag{7a}$$

$$\mathbf{R}_{\tilde{\mathbf{g}}_{b,a}^t}^{\mathrm{robust}} = \boldsymbol{\Delta}^{\mathrm{robust}} + \mathbf{R}_{\tilde{\mathbf{g}}_{b,a}^t}^{\mathrm{MMSE}}, \tag{7b}$$

$$\mathbf{R}_{\tilde{\mathbf{g}}_{b,a}^t}^{\mathrm{LS}} = \frac{\sigma_n^2}{p^u}\mathbf{B}^{-1}, \tag{7c}$$

where $\mathbf{B} = \mathbf{X}^H\mathbf{X} = \begin{pmatrix} \mathbf{P}_{1,1} & \mathbf{Q}_{2,1}^H \\ \mathbf{Q}_{2,1} & \mathbf{P}_{2,2} \end{pmatrix}$, $\mathbf{P}_{m,m} = \mathbf{X}_{m,b}^H\mathbf{X}_{m,b} = \mathbf{F}^H\boldsymbol{\Phi}_{m,b}^H\mathbf{T}_m^H\mathbf{T}_m\boldsymbol{\Phi}_{m,b}\mathbf{F}$ is the equivalent auto-correlation matrix of the training sequence for MS $m$, $m = 1, 2$, $\mathbf{Q}_{2,1} = \mathbf{X}_{2,b}^H\mathbf{X}_{1,b} = \mathbf{F}^H\boldsymbol{\Phi}_{2,b}^H\mathbf{T}_2^H\mathbf{T}_1\boldsymbol{\Phi}_{1,b}\mathbf{F}$ is the equivalent cross-correlation matrix of the training sequences of MS 1 and MS 2, and $\boldsymbol{\Delta}^{\mathrm{robust}} = \frac{\sigma_n^2}{p^u}(\mathbf{B} + \frac{\sigma_n^2}{p^u}\mathbf{D}_{b,a}^{-1})^{-1}\mathbf{B}(\mathbf{I}_{ML} - \mathbf{R}_{b,a}\mathbf{D}_{b,a}^{-1})(\mathbf{B} + \frac{\sigma_n^2}{p^u}\mathbf{D}_{b,a}^{-1})^{-1} + \mathbf{R}_{b,a}\mathbf{B}[(\mathbf{B} + \frac{\sigma_n^2}{p^u}\mathbf{R}_{b,a}^{-1})^{-1} - (\mathbf{B} + \frac{\sigma_n^2}{p^u}\mathbf{D}_{b,a}^{-1})^{-1}]$.

To further simplify our analysis and gain some insight into the problem, we assume uniform PDP of the small scale fading channels. Then the MMSE estimator degenerates to the robust estimator. From (7a), the MSE for MMSE estimator is derived as (see Appendix A for details)

$$\mathrm{MSE}_{m,b,a}^{\mathrm{MMSE}} = \eta_{m,b}\frac{\sigma_n^2}{p^u}\frac{1}{K}\sum_{l=0}^{L-1} f_{\mathrm{MMSE}}(\lambda_l),\ m = 1, 2, \tag{8}$$

where $\eta_{m,b} = 1/(1 + \frac{\sigma_n^2}{\alpha_{m,b}^2 p^u}\frac{L}{K})$, $f_{\mathrm{MMSE}}(\lambda_l) = \frac{1}{1-\beta\lambda_l^2}$, $\beta = 1/\prod_{j=1}^{2}(1 + \frac{\sigma_n^2}{\alpha_{j,b}^2 p^u}\frac{L}{K})$ and $\lambda_l^2$ is the $l$th eigenvalue of $\frac{\mathbf{Q}_{2,1}^H\mathbf{Q}_{2,1}}{K^2}$, $0 \le \lambda_l^2 < 1$.

From (7c), the MSE for LS estimator can be derived as (see Appendix B for details)

$$\mathrm{MSE}_{m,b,a}^{\mathrm{LS}} = \frac{\sigma_n^2}{p^u}\frac{1}{K}\sum_{l=0}^{L-1} f_{\mathrm{LS}}(\lambda_l),\ m = 1, 2, \tag{9}$$

where $f_{\mathrm{LS}}(\lambda_l) = \frac{1}{1-\lambda_l^2}$.

To minimize the MSE of the estimators, the matrix $\mathbf{B}$ should be a diagonal matrix [19]. This requires that C1) $\mathbf{P}_{mm}$ is diagonal, which can be satisfied when $\mathbf{T}_m^H \mathbf{T}_m = \mathbf{I}_K$, and C2) $\mathbf{Q}_{2,1} = \mathbf{0}$, which demands the training sequences of the MSs in two cells to be orthogonal.

The condition C1) holds when the training sequences have perfect auto-correlation. When the virtual carriers (VC) in practical OFDM systems are considered or the training sequences are not sent on all subcarriers with equi-power and equi-spaced, C1) does not hold any more.

To ensure C2), the training sequences for the MSs in different cells should be orthogonal. This can be implemented in time or frequency domain, but the resources occupied by training will increase linearly with the number of MSs. Phase shift orthogonalization, where two sequences are orthogonal when their relative phase shift is larger than $\frac{2\pi}{K}L$, is known as an efficient way to generate training sequence with perfect cross-correlation [8, 19]. At most $\lfloor K/L \rfloor$ orthogonal sequences can be constructed from a sequence.

Considering the propagation delay in multi-cell scenarios, to construct the phase shift orthogonal training sequences, the relative phase shift of the two sequences for two MSs should exceed $\frac{2\pi}{K}\bar{L}$, where $\bar{L} = L + l_{delay}$ and $l_{delay} = \lceil \frac{\tau_{m,b}-\tau_{i,b}}{T_s} \rceil$ represents the sampled propagation delay difference. Then, the maximum number of orthogonal training sequences that can be constructed is $\lfloor K/\bar{L} \rfloor$. When all MSs are located in one cell, $l_{delay}$ is much smaller than $L$ in typical outdoor channels[2]. By contrast, if the MSs are scattered in multiple cells, $l_{delay}$ will be comparable to the multipath delay. Consequently, few orthogonal training sequences are available for a given sequence length since $\bar{L}$ is large. This again leads to low spectrum efficiency. Furthermore, the inter-cell orthogonality demands inter-cell signalling and protocol to coordinate the training resources[3], which will become a burden when the coordinated clusters are formed dynamically.

In the following, we will analyze the performance loss led by the non-orthogonal training. To highlight the impact of the non-orthogonal training sequences for the MSs in different cells, we assume that the condition C1) holds.

---

[2] Take the urban macro channel in systems complying Long Term Evolution (LTE) standard as an example, the multipath delay is usually $4 \sim 5\mu$s. If we consider the cell radius to be $250$m, then the maximum delay difference is $0.7\mu$s, which is negligible compared to the multipath delay.

[3] In practical cellular systems such as those complying LTE standard, partial band may be used for uplink training to increase the power spectrum density for cell edge MSs [20]. When there is no inter-cell coordination, the training signals may overlap partially in the frequency domain, which will increase the cross-correlation of the training signals [21].

### B. Impact of Non-Orthogonal Training

For comparison, we first assume that the training sequences of MSs in different cells are orthogonal, i.e., $\mathbf{Q}_{2,1} = \mathbf{0}$. Then the values of $\lambda_l$, $l = 0, \cdots, L-1$, in (8) and (9) are zeros, and we can see the MSE for estimating the local and the cross channels. In this case, both $f_{\text{LS}}(\lambda_l)$ and $f_{\text{MMSE}}(\lambda_l)$ are equal to $1$, and the MSE of MMSE and LS estimators[4] are

$$\text{MSE}_{m,b,a}^{\text{MMSE}} = \frac{1}{1 + \frac{\sigma_n^2}{\alpha_{m,b}^2 p^u} \frac{L}{K}} \frac{\sigma_n^2}{p^u} \frac{L}{K}, \tag{10a}$$

$$\text{MSE}_{m,b,a}^{\text{LS}} = \frac{\sigma_n^2}{p^u} \frac{L}{K}. \tag{10b}$$

For the LS estimator, the MSE of the composite CIR estimate, $\hat{\mathbf{g}}_{m,b,a}^t$, depends on $\sigma_n^2$. We assume that the noise variance at all BSs are the same. Then the MSE of $\hat{\mathbf{g}}_{m,b,a}^t$ for $b = 1, \cdots, B$ are identical, no matter they are the local or the cross channels of MS $m$. For the MMSE estimator, the MSE of $\hat{\mathbf{g}}_{m,b,a}^t$ depends on $\alpha_{m,b}^2$ as well, which is the large scale fading energy of $\mathbf{g}_{m,b,a}^t$. If MS $m$ is in the same cell as BS $c_m$, then $\mathbf{g}_{m,c_m,a}^t$ is the local composite channel for MS $m$ while $\mathbf{g}_{m,b,a}^t$ for $b \neq c_m$ are its cross composite channels. Since the local channel energy $\alpha_{m,c_m}^2$ is usually larger than the cross channel energy $\alpha_{m,b}^2$, $b \neq c_m$, we can observe from (10a) that the MSE of the weak cross channels is even less than that of the strong local channels.

At the first glance, this conclusion is inconsistent with the conventional understanding, where the MSE of the estimates of the cross channels should be larger than that of local channels. Nevertheless, this understanding is only applicable for estimating the small scale fading channels whose average energy is 1. To see this, we normalize the MSE of $\hat{\mathbf{g}}_{m,b,a}^t$ by $\alpha_{m,b}^2$ to obtain a normalized MSE (NMSE) of $\hat{\mathbf{g}}_{m,b,a}^t$, which is actually the MSE for estimating the small scale fading channel $\hat{\mathbf{h}}_{m,b,a}^t$. The NMSE for both MMSE and LS estimators can be expressed as follows

$$\text{NMSE}_{m,b,a}^{\text{MMSE}} = \frac{1}{1 + \frac{\sigma_n^2}{\alpha_{m,b}^2 p^u} \frac{L}{K}} \frac{\sigma_n^2}{\alpha_{m,b}^2 p^u} \frac{L}{K}, \tag{11a}$$

$$\text{NMSE}_{m,b,a}^{\text{LS}} = \frac{\sigma_n^2}{\alpha_{m,b}^2 p^u} \frac{L}{K}. \tag{11b}$$

It follows that the MSE of the estimates for the small scale fading channels with low receive energy is larger than that with high receive energy.

---

[4] Again we assume unform PDP in this subsection.

When the training sequences of MSs in different cells are not orthogonal, then $\lambda_l^2 \neq 0$, and both $f_{\mathrm{LS}}(\lambda_l)$ and $f_{\mathrm{MMSE}}(\lambda_l)$ exceed $1$.

From the expression of $f_{\mathrm{LS}}(\lambda_l)$, we can see that if $\lambda_l^2$ is close to $1$ for any $l$, its value will be extremely large and the estimation performance will be severely degraded. This means that the LS estimator is quite sensitive to the orthogonality of the training sequences.

In the expression of $f_{\mathrm{MMSE}}(\lambda_l)$, $\lambda_l^2$ is weighted by $\beta$, whose value is always less than $1$. If two MSs are all in the same cell, $\alpha_{j,b}^2$ is generally large, then $\beta$ is close to $1$ and $f_{\mathrm{MMSE}}(\lambda_l) \approx f_{\mathrm{LS}}(\lambda_l)$. This implies if the MSs in the same cell use non-orthogonal training sequences, the performance of the MMSE estimator will degrade severely. On the other hand, if two MSs are in different cells, since the large scale channel gains from MSs to their non-serving BSs are low that leads to small $\beta$, $f_{\mathrm{MMSE}}(\lambda_l)$ will not be too large even if $\lambda_l^2$ is close to 1. This indicates that the MMSE estimator is robust to the non-orthogonality of the training sequences in different cells, thanks to the severe energy attenuation of the channels from MSs to their non-serving BSs.

Note that this conclusion holds for both MSE and NMSE since they only differ in a constant.

### *C. Performance Gap between MMSE Estimator and Robust Estimator*

In wideband cellular systems, the PDP is in fact not uniform. Then the robust estimator will be inferior to the MMSE estimator. Nevertheless, we will show in the following analysis that the performance gap between the two estimators is minor when the training sequences are orthogonal. We will show through simulations in Section VI that the same conclusion can be drawn when the training sequences are not orthogonal.

When the training sequences are orthogonal, $\mathbf{B} = \mathbf{X}^H\mathbf{X} = K\mathbf{I}_{2L}$. Substituting $\mathbf{B}$ into (7a) and (7b), we can derive the MSE difference of the MMSE estimator and robust estimator as

$$\Delta_{m,b,a}^{\mathrm{MMSE}} = \sum_{i=(m-1)L+1}^{mL} \left[\mathbf{R}_{\tilde{\mathbf{g}}_{b,a}}^{\mathrm{robust}}(i,i) - \mathbf{R}_{\tilde{\mathbf{g}}_{b,a}}^{\mathrm{MMSE}}(i,i)\right] = \alpha_{m,b}^2 \left(\sum_{l=0}^{L-1} \frac{\sigma_{h_l}^4}{\sigma_{h_l}^2 + \mu} - \frac{1}{1+\mu L}\right), \quad (12)$$

where $\mu = \frac{\sigma_n^2}{\alpha_{m,b}^2 p^u K}$, $\sigma_{h_l}^2$ is the variance of the $l$th resolvable path of small scale fading channel.

When $\alpha_{m,b}^2$ is large enough, $\mu$ approaches to $0$ and $\Delta_{m,b,a}^{\mathrm{MMSE}}$ approaches to $0$ also. On the other hand, when $\alpha_{m,b}^2$ decreases, $\mu$ will increase, but $\Delta_{m,b,a}^{\mathrm{MMSE}}$ will still be fairly small. That is to say, in the asymmetric channels, the robust estimator performs closely to the MMSE estimator.

## V. IMPACT OF CHANNEL ESTIMATION ERRORS ON COOPERATIVE TRANSMISSION

In this section, we first analyze the average per MS rate loss led by the channel estimation errors with CoMP transmission using ZFBF. Then, we obtain a lower bound of the average achievable rate when the MMSE estimator is applied.

### *A. CFR Estimation Errors*

Since composite CFR is required for precoding in OFDM systems, we need to transform the MSE of CIR estimate to the MSE of CFR estimate at each subcarrier, $\sigma^2_{e_{m,b,a}}(k)$, $k = 0, \cdots, K-1$. Denote the sum MSE of CFR at all subcarriers as $\mathbb{E}\{\|\tilde{\mathbf{g}}^f_{m,b,a}\|^2\} = \mathbb{E}\{\|\mathbf{g}^f_{m,b,a} - \hat{\mathbf{g}}^f_{m,b,a}\|^2\}$. It can be obtained from the MSE of CIRs provided in previous sections as follows,

$$\mathbb{E}\{\|\tilde{\mathbf{g}}^f_{m,b,a}\|^2\} = \mathbb{E}\{\|\mathbf{F}_{m,b}\mathbf{g}^t_{m,b,a} - \mathbf{F}_{m,b}\hat{\mathbf{g}}^t_{m,b,a}\|^2\} = \mathbb{E}\{\|\mathbf{F}_{m,b}\tilde{\mathbf{g}}^t_{m,b,a}\|^2\} \overset{(a)}{=} K\mathrm{MSE}_{m,b,a}, \tag{13}$$

where (a) comes from the fact that $\mathbf{F}^H_{m,b}\mathbf{F}_{m,b} = \mathbf{F}^H\mathbf{\Phi}^H_{m,b}\mathbf{\Phi}_{m,b}\mathbf{F} = K\mathbf{I}_L$. When the training sequences of all MSs are orthogonal and the resolvable multipaths are uncorrelated, the MSE of the CFR at each subcarrier can be obtained as [17]

$$\sigma^2_{e_{m,b,a}}(k) = \mathbb{E}\{\|\tilde{\mathbf{g}}^f_{m,b,a}\|^2\}/K = \mathrm{MSE}_{m,b,a},\ k = 0, \cdots, K-1. \tag{14}$$

From (8) and (9) we know that the MSE of the CIR estimates between all antennas of BS $b$ and MS $m$ are the same, which results in $\sigma^2_{e_{m,b,a}} = \sigma^2_{e_{m,b}}$, $a = 1, \cdots, N_t$. The composite CFR between BS $b$ and MS $m$ at the $k$th subcarrier can be modeled as $\mathbf{g}^f_{m,b}(k) = \hat{\mathbf{g}}^f_{m,b}(k) + \tilde{\mathbf{g}}^f_{m,b}(k)$, where $\mathbf{g}^f_{m,b}(k) = [g^f_{m,b,1}(k), \cdots, g^f_{m,b,N_t}(k)]^H$, $\hat{\mathbf{g}}^f_{m,b}(k)$ is the estimation of $\mathbf{g}^f_{m,b}(k)$ and $\tilde{\mathbf{g}}^f_{m,b}(k)$ is the estimation error vector whose covariance is $\sigma^2_{e_{m,b}}(k)\mathbf{I}_{N_t}$. Since the transmission procedures of all subcarriers are same, the index of subcarrier is omitted in the following for brevity.

### *B. Impact of Channel Estimation Errors on CoMP Transmission*

When the global channel vectors are reconstructed at the CU from the estimates provided by all coordinated BSs, a multicell ZFBF is computed as follows

$$\mathbf{V} = (\hat{\mathbf{G}}^f)^H\left[\hat{\mathbf{G}}^f(\hat{\mathbf{G}}^f)^H\right]^{-1}. \tag{15}$$

Then the beamforming vector of all cooperative BSs for MS $m$ is obtained by normalizing the $m$th column of $\mathbf{V}$ as $\mathbf{v}_m = \mathbf{V}(:,m)/\|\mathbf{V}(:,m)\|$ and $\mathbf{v}_m = [(\mathbf{v}_{1,m})^H, \cdots, (\mathbf{v}_{B,m})^H]^H$, where $\mathbf{v}_{b,m} \in \mathbb{C}^{N_t\times 1}$ is the precoder vector of BS $b$ for MS $m$.

In order to derive a closed-form expression of the per MS rate loss led by the channel estimation errors, we assume that the number of MSs cooperatively served by $B$ BSs is $BN_t$, which indicates full multiplexing CoMP-MU transmission as in [22]. We further assume that the power allocated to all MSs are identical, which is denoted as $p^d$.

The average rate of MS $m$ achieved by CSI estimate-based ZFBF is obtained from (2) as

$$R_m = \mathbb{E}\left\{\log_2(1+\mathrm{SINR}_m)\right\} = \mathbb{E}\left\{\log_2\left(1+\frac{p^d|\mathbf{g}_m^H\mathbf{v}_m|^2}{\sigma_z^2+p^d\sum_{j=1,j\neq m}^{M}|\mathbf{g}_m^H\mathbf{v}_j|^2}\right)\right\}. \tag{16}$$

The average rate of MS $m$ achieved by perfect CSI-based ZFBF is given by

$$R_m^{\mathrm{Ideal}} = \mathbb{E}\left\{\log_2\left(1+\frac{p^d}{\sigma_z^2}|\mathbf{g}_m^H\mathbf{v}_m^{\mathrm{Ideal}}|^2\right)\right\}, \tag{17}$$

where $\mathbf{v}_m^{\mathrm{Ideal}} = [(\mathbf{v}_{1,m}^{\mathrm{Ideal}})^H,\cdots,(\mathbf{v}_{B,m}^{\mathrm{Ideal}})^H]^H$ is the perfect CSI-based ZFBF vector of all BSs for MS $m$, which is chosen to be orthogonal to $\mathbf{g}_j$ for $j=1,\cdots,M$ and $j\neq m$.

**Theorem 1** The rate loss of MS $m$ of the CoMP transmission using ZFBF led by the channel estimation errors can be upper bounded by

$$\Delta R_m = R_m^{\mathrm{Ideal}} - R_m < \log_2\left(1+\frac{p^d}{\sigma_z^2}\mathbb{E}\{I_m\}\right) = \Delta R_m^{\mathrm{UB}}, \tag{18}$$

where $I_m = \sum_{j=1,j\neq m}^{M}|(\tilde{\mathbf{g}}_m^f)^H\mathbf{v}_j|^2$ is the average interference power experienced by MS $m$, $\tilde{\mathbf{g}}_m^f = [(\tilde{\mathbf{g}}_{m,1}^f)^H,\cdots,(\tilde{\mathbf{g}}_{m,B}^f)^H]^H$ is the estimation error vector of the global channel vector $\mathbf{g}_m^f$.

The derivation is similar to that in [22]. Due to the lack of space, we omit the proof of the Theorem. From (18), the achievable rate of MS $m$ when estimated CSI are used for CoMP transmission can be lower bounded by

$$R_m > R_m^{\mathrm{Ideal}} - \Delta R_m^{\mathrm{UB}}. \tag{19}$$

To gain further insight into the rate loss, we assume that the channel estimation errors $\tilde{\mathbf{g}}_m^f$ are independent of the precoder vectors $\mathbf{v}_j$ for $j=1,\cdots,M$ and $j\neq m$. This assumption is satisfied when the MMSE estimator is applied. When MMSE estimator is used, since the channel estimation errors are independent of the channel estimates, and the precoders are functions of the channel estimates, the channel estimation errors and the precoders are mutually independent. In Section VI, we will examine the impact of estimation errors led by the LS and robust estimators on CoMP transmission through simulations.

As stated in Section V-A, the MSEs of the CFRs between MS $m$ and all antennas of BS $b$ are identical, then the rate loss upper bound of MS $m$ can be further derived as follows by taking expectation over the channel estimation errors (see Appendix C for details)

$$\Delta R_m^{\mathrm{UB}} = \log_2[1 + \sum_{j=1,j\neq m}^{M} \sum_{b=1}^{B} \underbrace{\frac{\alpha_{m,b}^2 p^d}{\sigma_z^2}}_{\mathrm{SNR}_{m,b}^d} \underbrace{\frac{\sigma_{e_{m,b}}^2}{\alpha_{m,b}^2}}_{\mathrm{NMSE}_{m,b}} \|\mathbf{v}_{b,j}\|^2]. \tag{20}$$

**Remark 1** To connect with the conventional understanding of the impact of the channel estimation errors, we show the contribution of channel estimation errors of the small scale fading channels, $\mathrm{NMSE}_{m,b}$, to the rate loss in (20), which is weighted by the downlink receive SNR of the link $\mathrm{SNR}_{m,b}^d$. For the local channels of MS $m$, i.e., $b = c_m$, $\mathrm{NMSE}_{m,c_m}$ is small and its contribution to the rate loss will be minor. For the cross channels of MS $m$, the estimation errors $\mathrm{NMSE}_{m,b}$ for $b \neq c_m$ will be large. However, because the receive SNRs of the cross links are considerably low, the impact of the channel estimation errors of cross channels will be significantly alleviated. This is true especially for cell center MSs.

Substituting the $\mathrm{NMSE}_{m,b}$ of the MMSE estimator under orthogonal training shown in (11a) into (20), we obtain the rate loss upper bound as follows

$$\Delta R_m^{\mathrm{UB}} = \log_2 \left[ 1 + \frac{p^d}{\sigma_z^2} \frac{\sigma_n^2}{p^u} \frac{L}{K} \sum_{j=1,j\neq m}^{M} \sum_{b=1}^{B} \frac{\|\mathbf{v}_{b,j}\|^2}{1 + \frac{\sigma_n^2}{\alpha_{m,b}^2 p^u} \frac{L}{K}} \right] \overset{(a)}{<} \log_2 \left[ 1 + (M-1) \frac{p^d}{\sigma_z^2} \frac{\sigma_n^2}{p^u} \frac{L}{K} \right], \tag{21}$$

where (a) is obtained because $\frac{1}{1+\frac{\sigma_n^2}{\alpha_{m,b}^2 p^u}\frac{L}{K}} < 1$, and $\sum_{b=1}^{B} \|\mathbf{v}_{b,j}\|^2 = 1$ as described in (15). $p^d$ and $p^u$ are respectively the power transmitted to each MS and that transmitted by each MS, $\sigma_z^2$ and $\sigma_n^2$ are the noise variances at the BS and MS. When $p^d$ and $p^u$ are fixed, the upper bound of the rate loss will not depend on the large scale fading gains of both local and cross channels.

According to (19) and (21), we can obtain the lower bound of the average rate achieved by MS $m$ under MMSE estimator and orthogonal training as

$$R_m > R_m^{\mathrm{Ideal}} - \log_2 \left[ 1 + (M-1) \frac{p^d}{\sigma_z^2} \frac{\sigma_n^2}{p^u} \frac{L}{K} \right] = R_m^{\mathrm{LB}}. \tag{22}$$

# VI. SIMULATION RESULTS

In this section, we compare the performance of different channel estimators and evaluate their impact on the performance of downlink CoMP system.

A cooperative cluster of two cells is considered ($B = 2$). The cell radius $r = 250$ m. Each BS has four omnidirectional antennas ($N_t = 4$), serving two single-antenna MSs. The downlink transmit power for each MS $p^d$ is $5$ dB larger than the uplink transmit power of each MS $p^u$. The maximum delay spread of the channel $\tau = 4\mu$s, and the channel is implemented as a tapped-delay line with Rayleigh fading coefficients and an exponential DPD with the attenuation factor being $1.4$. $K = 128$. The system bandwidth is $B = 5$ MHz, the sampling period is $T_s = 1/B = 0.2\mu$s, thus $L = \tau/T_s = 20$. Due to the lack of the space, we only present the performance of an OFDM system without VC and the training sequences are sent on full band. Extensive results show that the same conclusions can be drawn to the OFDM system with VC and the training sequences of MSs are sent on partial band.

The training sequences are constructed from Constant Amplitude Zero Autocorrelation Code (CAZAC) [23] as $t(k) = e^{-j\frac{\pi c n_k (n_k+1)}{N_{\text{ZC}}}}$, $k = 0, \cdots, K-1$, [20], where $N_{\text{ZC}} = 127$, $n_k = \text{mod}(k, N_{\text{ZC}})$. The training sequences for MSs in the same cell are orthogonal by cyclic shifting. The training sequences of MSs in different cells can be orthogonal or non-orthogonal. For orthogonal training, the training sequences for the four MSs in the two cells are constructed from the cyclic shift of the CAZAC with the same value of $c$. For non-orthogonal training, the training sequences of MSs in two cells use different values of $c$. The values of $c$ for two cells are set to $c_1 = 1$ and $c_2 = 7$, considering that their cross correlation is moderate.

## A. NMSEs of Different Estimators

To show the impact of MSs' positions on the estimation errors for small scale fading channels under orthogonal and non-orthogonal training for multiple MSs, we let the four MSs in the two cells be symmetrically located, as shown in Fig. 3. Then the channel estimation performance of all MSs are the same. We take the performance of one MS as an example to analyze.

In Fig. 4, the NMSEs versus local uplink receive SNR of three estimators for both local and cross channels are shown. When the training sequences are not orthogonal, the performance of the LS estimator degrades severely. By contrast, the performance gap of the MMSE estimator under orthogonal and non-orthogonal training is minor. Comparing the NMSE of the robust and

MMSE estimators, we observe that the performance loss of the robust estimator from the MMSE estimator is small. These results agree well with our previous analysis. Again, we should note that the impact of the non-orthogonal training sequences on the performance of estimating the small scale fading channels is the same as that of estimating the composite channels, since the MSE and NMSE only differ in a constant.

### *B. Downlink Average Rate with Different Channel Estimators*

*1) Positions of MSs are Fixed:* Now we verify the analysis in Section V, where the positions of the MSs in two cells are the same with before. We simulate the downlink average throughput of each MS, which is averaged over $1000$ realizations of small scale fading channels.

We first evaluate the tightness of the rate lower bound derived in Section V. The performance with MMSE estimator under orthogonal training is taken as an example. The per MS rate under the pefect ZFBF and the CSI estimate-based ZFBF are shown in Fig. 5, together with the lower bound of the achievable rate derived in (22). It shows that the derived lower bound is close to the rate obtained by simulation.

We then compare the impact of different estimators on the performance of CoMP transmission under both orthogonal and non-orthogonal training, which is shown in Fig. 6, where the throughputs under Non-CoMP transmission are also present as a reference. When the training sequences are orthogonal, the per MS throughputs under different estimators are almost the same. The performance gap from the perfect CSI-based ZFBF does not change no matter the MS is located at the cell edge or the cell center. When the training sequences of MSs in different cells are not orthogonal, the performance degradation when using both the MMSE and the robust estimators is minor. On contrary, the performance when using the LS estimator severely degrades, which is even worse than the Non-CoMP transmission. It indicates that the estimator can perform fairly well only when the large scale fading information is employed.

*2) Positions of MSs are Randomized:* Finally we simulate the case in which the locations of two MSs are randomly distributed in each cell. We use the average throughput per MS and the cell edge MS throughput as the performance metric. The results are shown in Fig. 7, which is obtained from $1000$ random drops. We can see that the same conclusion can be drawn as the case where the positions of MSs are fixed.

## VII. CONCLUSION

In this paper, we have studied the impact of *uplink channel asymmetry* on the performance of channel estimation and the impact of *downlink channel asymmetry* on the performance of BS cooperative transmission with channel estimation errors. We have analyzed three joint channel estimators, the MMSE estimator, a robust estimator and the LS estimator. Our analysis showed that if the training sequences of MSs in different cells are not orthogonal, the performance of estimating cross channels with the LS estimator severely degrades. By contrast, the MMSE estimator is robust to the non-orthogonal training, and due to the *uplink channel asymmetry* the robust estimator has minor performance loss. By analyzing the impact of channel estimation errors on the cooperative ZFBF transmission, we showed that due to the *downlink channel asymmetry*, the contribution of the channel estimation errors to the rate loss is weighted by the receive SNRs of the corresponding links. As a result, despite that the estimation errors of the small scale fading channels of the cross links are large, their impact on the rate loss is minor. When the joint channel estimators exploit the large scale fading gains, CoMP transmission performs fairly well, even without inter-cell orthogonal training. This improves the spectral efficiency and simplify the inter-cell signalling required to coordinate the training resources.

## APPENDIX A

## DERIVATION OF THE MSE OF MMSE ESTIMATOR

Assume uniform PDP for small scale fading channels, i.e., $\mathbf{R}_{b,a} = diag\{[\alpha_{1,b}^2 \frac{1}{L}\mathbf{I}_L, \alpha_{2,b}^2 \frac{1}{L}\mathbf{I}_L]\}$. Substituting the expression of $\mathbf{B}$ to (7a) and applying the formula of block matrix inversion, the covariance matrix of the estimation errors becomes

$$\mathbf{R}_{\tilde{\mathbf{g}}_{b,a}}^{\mathrm{MMSE}} = \frac{\sigma_n^2}{p^u K} \begin{pmatrix} \mathbf{N} & -\eta_{b,2}\mathbf{N}\frac{\mathbf{Q}_{21}^H}{K} \\ -\eta_{b,2}\frac{\mathbf{Q}_{21}}{K}\mathbf{N} & (\eta_{b,2})^2 \frac{\mathbf{Q}_{21}}{K}\mathbf{N}\frac{\mathbf{Q}_{21}^H}{K} + \eta_{b,2}\mathbf{I}_L \end{pmatrix}, \tag{23}$$

where $\mathbf{N} = \left(\frac{1}{\eta_{b,1}}\mathbf{I}_L - \eta_{b,2}\frac{\mathbf{Q}_{21}^H\mathbf{Q}_{21}}{K^2}\right)^{-1}$, $\eta_{b,m} = \frac{\alpha_{b,m}^2}{\alpha_{b,m}^2 + \frac{L\sigma_n^2}{K}}$.

The MSE of the MMSE estimator for CIR from the MS $1$ to antenna $a$ of BS $b$ is

$$\begin{aligned} \mathrm{MSE}_{1,b,a}^{\mathrm{MMSE}} = \frac{\sigma_n^2}{p^u K} tr\{\mathbf{N}\} = \eta_{b,1}\frac{\sigma_n^2}{p^u K} tr\left\{\left(\mathbf{I}_L - \eta_{b,1}\eta_{b,2}\frac{\mathbf{Q}_{21}^H\mathbf{Q}_{21}}{K^2}\right)^{-1}\right\} \\ \overset{(a)}{=} \eta_{b,1}\frac{\sigma_n^2}{p^u K}\sum_{l=0}^{L-1}\frac{1}{1-\lambda_l^2\prod_{j=1}^{2}\eta_{b,j}}, \end{aligned} \tag{24}$$

where (a) follows from applying the eigenvalue decomposition as $\frac{\mathbf{Q}_{21}^H\mathbf{Q}_{21}}{K^2} = \mathbf{U}\mathbf{\Lambda}\mathbf{U}^H$, $\mathbf{U}$ is an unitary matrix and $\mathbf{\Lambda} = \mathrm{diag}\{[\lambda_0^2, \cdots, \lambda_{L-1}^2]\}$.

The MSE of MMSE estimator for CIR from the MS $2$ can be derived as

$$\begin{aligned}\mathrm{MSE}_{2,b,a}^{\mathrm{MMSE}} =& \frac{\sigma_n^2}{p^u K} tr\left\{\eta_{b,2}^2 \frac{\mathbf{Q}_{21}}{K}\mathbf{N}\frac{\mathbf{Q}_{21}^H}{K} + \eta_{b,2}\mathbf{I}_L\right\} \\ =& \frac{\sigma_n^2}{p^u K}\eta_{b,2}^2 tr\left\{\left(\frac{1}{\eta_{b,1}}\mathbf{I}_L - \eta_{b,2}\frac{\mathbf{Q}_{21}^H\mathbf{Q}_{21}}{K^2}\right)^{-1}\frac{\mathbf{Q}_{21}^H}{K}\frac{\mathbf{Q}_{21}}{K}\right\} + \frac{\sigma_n^2}{K}\eta_{b,2} tr\left\{\mathbf{I}_L\right\} \\ =& \frac{\sigma_n^2}{p^u K}\eta_{b,2}^2\eta_{b,1}\sum_{l=0}^{L-1}\frac{\lambda_l^2}{1-\lambda_l^2\eta_{b,1}\eta_{b,2}} + \frac{\sigma_n^2}{K}\eta_{b,2}L = \eta_{b,2}\frac{\sigma_n^2}{p^u K}\sum_{l=0}^{L-1}\frac{1}{1-\lambda_l^2\prod_{j=1}^{2}\eta_{b,j}}. \end{aligned} \tag{25}$$

Comparing (24) and (25), we can see that the only difference is the factor $\eta_{b,m}$. The channel that experiences large attenuation exhibits small estimate errors.

## APPENDIX B

## DERIVATION OF THE MSE OF LS ESTIMATOR

Substituting the expression of $\mathbf{B}$ into (7c) and using the formula of $2\times 2$ block matrix inversion, we can derive the covariance matrix of the estimator errors as

$$\mathbf{R}_{\tilde{\mathbf{g}}_{b,a}}^{\mathrm{LS}} = \frac{\sigma_n^2}{p^u K}\begin{pmatrix} \mathbf{M} & -\mathbf{M}\frac{\mathbf{Q}_{21}^H}{K} \\ -\frac{\mathbf{Q}_{21}}{K}\mathbf{M} & \frac{\mathbf{Q}_{21}}{K}\mathbf{M}\frac{\mathbf{Q}_{21}^H}{K} + \mathbf{I}_L \end{pmatrix}, \tag{26}$$

where $\mathbf{M} = \left(\mathbf{I}_L - \frac{\mathbf{Q}_{21}^H\mathbf{Q}_{21}}{K^2}\right)^{-1}$.

The MSE of the LS estimator for the CIR from MS $1$ to antenna $a$ of BS $b$ can be derived as

$$\mathrm{MSE}_{1,b,a}^{\mathrm{LS}} = \frac{\sigma_n^2}{p^u K} tr\{\mathbf{M}\} = \frac{\sigma_n^2}{p^u K} tr\left\{\left(\mathbf{I}_L - \mathbf{U}\mathbf{\Lambda}\mathbf{U}^H\right)^{-1}\right\} = \frac{\sigma_n^2}{p^u K}\sum_{l=0}^{L-1}\frac{1}{1-\lambda_l^2}. \tag{27}$$

The MSE of LS estimator for CIR from the MS $2$ can be derived in the same way as

$$\begin{aligned}\mathrm{MSE}_{2,b,a}^{\mathrm{LS}} &= \frac{\sigma_n^2}{p^u K} tr\left\{\frac{\mathbf{Q}_{21}}{K}\mathbf{M}\frac{\mathbf{Q}_{21}^H}{p^u K} + \mathbf{I}_L\right\} \\ &= \frac{\sigma_n^2}{p^u K} tr\left\{\left(\mathbf{I}_L - \frac{\mathbf{Q}_{21}^H\mathbf{Q}_{21}}{K^2}\right)^{-1}\frac{\mathbf{Q}_{21}^H}{K}\frac{\mathbf{Q}_{21}}{K}\right\} + \frac{\sigma_n^2}{K} tr\{\mathbf{I}_L\} = \frac{\sigma_n^2}{p^u K}\sum_{l=0}^{L-1}\frac{1}{1-\lambda_l^2}. \end{aligned} \tag{28}$$

Comparing (27) and (28), we find that the MSEs of the LS estimator for the CIRs from different MSs are identical.

## APPENDIX C

## RATE LOSS AFTER TAKEN EXPECTATION OVER CHANNEL ESTIMATION ERRORS

The average interference power experienced by MS $m$ in (18) can be derived by taking expectation with respect to the estimation errors, i.e.,

$$\begin{aligned}
\mathbb{E}\{I_m\} &= \mathbb{E}_{\tilde{\mathbf{g}}_m^f}\left\{\sum_{j=1,j\neq m}^{M}\left|(\tilde{\mathbf{g}}_m^f)^H\mathbf{v}_j\right|^2\right\} = \sum_{j=1,j\neq m}^{M}\mathbb{E}_{\tilde{\mathbf{g}}_m^f}\left\{\left|\sum\nolimits_{b=1}^{B}(\tilde{\mathbf{g}}_{m,b}^f)^H\mathbf{v}_{b,j}\right|^2\right\}\\
&= \sum_{j=1,j\neq m}^{M}\mathbb{E}_{\tilde{\mathbf{g}}_m^f}\left\{\sum\nolimits_{b=1}^{B}\left|(\tilde{\mathbf{g}}_{m,b}^f)^H\mathbf{v}_{b,j}\right|^2 + 2\Re\left\{\sum\nolimits_{t=1}^{B}\sum\nolimits_{u=1,u\neq t}^{B}(\tilde{\mathbf{g}}_{m,t}^f)^H\mathbf{v}_{t,j}(\mathbf{v}_{u,j})^H\tilde{\mathbf{g}}_{j,u}^f\right\}\right\}\\
&\overset{(a)}{=} \sum_{j=1,j\neq m}^{M}\sum_{b=1}^{B}\mathbb{E}_{\tilde{\mathbf{g}}_m^f}\left\{\left|(\tilde{\mathbf{g}}_{m,b}^f)^H\mathbf{v}_{b,j}\right|^2\right\}\\
&\overset{(b)}{=} \sum_{j=1,j\neq m}^{M}\sum_{b=1}^{B}\sigma_{e_{m,b}}^2\|\mathbf{v}_{b,j}\|^2,
\end{aligned} \tag{29}$$

where $(a)$ follows because the channel estimation errors of the channels from multiple BSs to one MS are assumed to be uncorrelated and their expectations are zero. $(b)$ is derived by considering that the covariance of estimation errors for the channels from multiple antennas of one BS are the same, i.e., $\mathbb{E}\{\tilde{\mathbf{g}}_{m,b}^f(\tilde{\mathbf{g}}_{m,b}^f)^H\} = \sigma_{e_{m,b}}^2\mathbf{I}_{N_t}$.

Substituting (29) into (18), we can get the upper bound of the rate loss under CoMP transmission as

$$\begin{aligned}
\Delta R_m^{\mathrm{UB}} &= \log_2\left[1+\frac{p^d}{\sigma_z^2}\sum_{j=1,j\neq m}^{M}\sum_{b=1}^{B}\sigma_{e_{m,b}}^2\|\mathbf{v}_{b,j}\|^2\right]\\
&= \log_2\left[1+\sum_{j=1,j\neq m}^{M}\sum_{b=1}^{B}\frac{\alpha_{m,b}^2p^d}{\sigma_z^2}\frac{\sigma_{e_{m,b}}^2}{\alpha_{m,b}^2}\|\mathbf{v}_{b,j}\|^2\right].
\end{aligned} \tag{30}$$

## REFERENCES

[1] M. K. Karakayali, G. J. Foschini, and R. A. Valenzuela, “Network coordination for spectrally efficient communications in cellular systems,” *IEEE Wireless Commun. Mag.*, vol. 13, no. 4, pp. 56–61, Aug. 2006.

[2] A. Tölli, M. Codreanu, and M. Juntti, “Cooperative MIMO-OFDM cellular system with soft handover between distributed base station antennas,” *IEEE Trans. Wireless Commun.*, vol. 7, no. 4, pp. 1428–1440, Apr. 2008.

[3] J. Jose, A. Ashikhmin, T. Marzetta, and S. Vishwanath, “Pilot contamination problem in multi-cell TDD systems,” in *Proc. IEEE Int. Symp. Information Theory (ISIT)*, Seoul, Korea, June 2009, pp. 2184–2188.

[4] G. Kang, P. Hasselbach, Y. Yang, P. Zhang, and A. Klein, “Pilot design for inter-cell interference mitigation in MIMO OFDM system,” *IEEE Commun. Lett.*, vol. 11, no. 3, pp. 237–239, Mar. 2007.

[5] D. Katselis, E. Kofidis, and S. Theodoridis, “On training optimization for estimation of correlated MIMO channels in the presence of multiuser interference,” *IEEE Trans. Signal Processing*, vol. 56, no. 10, pp. 4892–4904, Oct. 2008.

[6] S. Lee, K. Kwak, J. Kim, and D. Hong, “Channel estimation approach with variable pilot density to mitigate interference over time-selective cellular OFDM systems,” *IEEE Trans. Wireless Commun.*, vol. 7, no. 7, pp. 2694–2704, July 2008.

[7] M. R. Raghavendra, S. Bhashyam, and K. Giridhar, “Interference rejection for parametric channel estimation in reuse-1 cellular OFDM systems,” *IEEE Trans. Veh. Technol.*, vol. 58, no. 8, pp. 4342–4352, Oct. 2009.

[8] Y. Li, “Simplified channel estimation for OFDM systems with multiple trasnmit antennas,” *IEEE Trans. Commun.*, vol. 1, no. 1, pp. 67–75, Jan. 2002.

[9] H. S. Kim, S. H. Lee, and Y. H. Lee, “Channel sounding for multi-sector cooperative beamforming in TDD-OFDM wireless systems,” in *Proc. IEEE Int. Conf. Commun. (ICC)*, Cape Town, South Africa, May 2010.

[10] A. Papadogiannis, D. Gesbert, and E. Hardouin, “A dynamic clustering approach in wireless networks with multi-cell cooperative processing,” in *Proc. IEEE Int. Conf. Commun. (ICC)*, Beijing, China, May 2008, pp. 4033–4037.

[11] M. S. L. Thiele, S. Schiffermuller, V. Jungnickel, and W. Zirwas, “Multi-cell channel estimation using virtual pilots,” in *Proc. IEEE Veh. Technol. Conf. Spring (VTC-S)*, Singapore, May 2008, pp. 1211–1215.

[12] T. Kwon, H. Song, and D. Hong, “Robust channel estimation in multicell OFDM(A) downlink systems with propagation delay,” in *Proc. IEEE Veh. Technol. Conf. Spring (VTC-S)*, Dublin, Ireland, May 2007, pp. 1450–1454.

[13] H. Zhang, N. B. Mehta, A. F. Molisch, J. Zhang, and H. Dai, “Asynchronous interference mitigation in cooperative base station systems,” *IEEE Trans. Wireless Commun.*, vol. 7, no. 1, pp. 155–165, Jan. 2008.

[14] S. Han, C. Yang, M. Bengtsson, and A. I. Perez-Neira, “Channel norm based user scheduling in coordinated multi-point systems,” in *Proc. IEEE Glob. Telecom. Conf. (GlobeCom)*, Nov. 2009.

[15] M. R. Raghavendra and K. Giridhar, “Improving channel estimation in OFDM systems for sparse multipath channels,” *IEEE Signal Processing Lett.*, vol. 12, no. 1, pp. 52–55, Jan. 2005.

[16] K. C. Hung and D. W. Lin, “Pilot-based LMMSE channel estimation for OFDM systems with power-delay profile approximation,” *IEEE Trans. Veh. Technol.*, vol. 59, no. 1, pp. 150–159, Jan. 2009.

[17] Y. Li, L. J. Cimini, and N. R. Sollenberger, “Robust channel estimation for OFDM systems with rapid dispersive fading channels,” *IEEE Trans. Commun.*, vol. 46, no. 7, pp. 902–915, July 1998.

[18] G. H. Golub and C. F. V. Loan, *Matrix Computations*. Baltimore MD: Johns Hopkins University Press, 1996.

[19] I. Barhumi, G. Leus, and M. Moonen, “Optimal training design for MIMO OFDM systems in mobile wireless channels,” *IEEE Trans. Signal Processing*, vol. 51, no. 6, pp. 1615–1624, June 2003.

[20] 3GPP Long Term Evolution (LTE), “Physical channels and modulation,” *TSG RAN TR 36.211 v8.4.0*, Sept. 2008.

[21] Y. Ogawa, T. Takata, T. Iwai, D. Imamura, K. Hiramatsu, and K. Miya, “Pilot signal generation scheme using frequency dependent cyclic shift sequence for inter-cell interference mitigation,” in *Proc. IEEE Radio and Wireless Symposium (RWS)*, San Diego, CA, Jan. 2009, pp. 421–424.

[22] G. Caire, N. Jindal, M. Kobayashi, and N. Ravindran, “Multiuser MIMO achievable rates with downlink training and channel state feedback,” *IEEE Trans. Inform. Theory*, vol. 56, no. 6, pp. 2845–2866, June 2010.

[23] D. C. Chu, “Polyphase codes with good periodic correlation properties,” *IEEE Trans. Inform. Theory*, vol. 18, no. 4, pp. 531–532, July 1972.

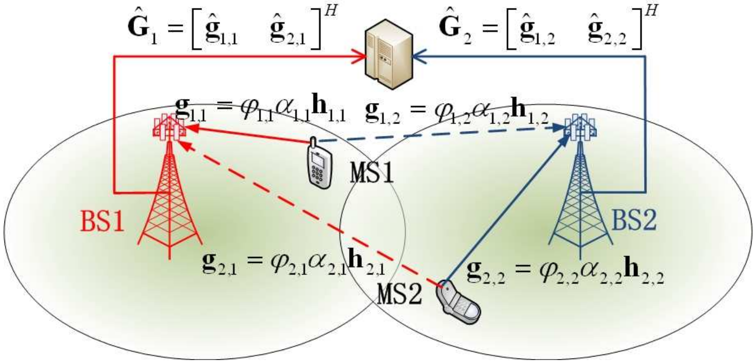
$\hat{\mathbf{G}}_1 = \left[\hat{\mathbf{g}}_{1,1} \quad \hat{\mathbf{g}}_{2,1}\right]^H$
$\hat{\mathbf{G}}_2 = \left[\hat{\mathbf{g}}_{1,2} \quad \hat{\mathbf{g}}_{2,2}\right]^H$
$\mathbf{g}_{1,1} = \varphi_{1,1}\alpha_{1,1}\mathbf{h}_{1,1}$
$\mathbf{g}_{1,2} = \varphi_{1,2}\alpha_{1,2}\mathbf{h}_{1,2}$
MS1
BS1
BS2
$\mathbf{g}_{2,1} = \varphi_{2,1}\alpha_{2,1}\mathbf{h}_{2,1}$
$\mathbf{g}_{2,2} = \varphi_{2,2}\alpha_{2,2}\mathbf{h}_{2,2}$
MS2

Fig. 1. Uplink training procedure of a two-cell CoMP system, where the solid lines denote the local channels and the dash lines represent the cross channels. The frequency domain channels are shown and the index of subcarrier is omitted for brevity.

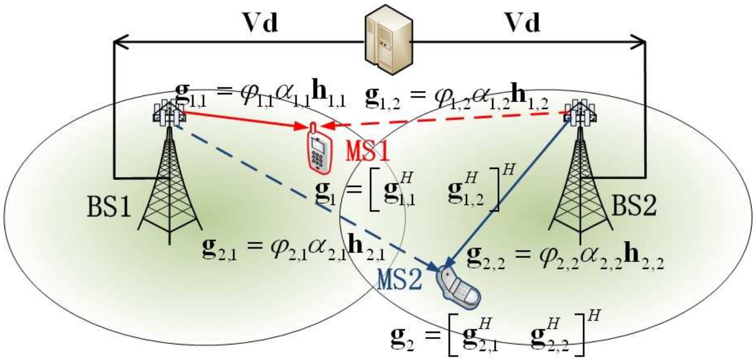
Vd
Vd
$\mathbf{g}_{1,1} = \varphi_{1,1}\alpha_{1,1}\mathbf{h}_{1,1}$
$\mathbf{g}_{1,2} = \varphi_{1,2}\alpha_{1,2}\mathbf{h}_{1,2}$
MS1
$\mathbf{g}_1 = \left[\mathbf{g}_{1,1}^H \quad \mathbf{g}_{1,2}^H\right]^H$
BS1
BS2
$\mathbf{g}_{2,1} = \varphi_{2,1}\alpha_{2,1}\mathbf{h}_{2,1}$
$\mathbf{g}_{2,2} = \varphi_{2,2}\alpha_{2,2}\mathbf{h}_{2,2}$
MS2
$\mathbf{g}_2 = \left[\mathbf{g}_{2,1}^H \quad \mathbf{g}_{2,2}^H\right]^H$

Fig. 2. Downlink transmission procedure of a two-cell CoMP system.

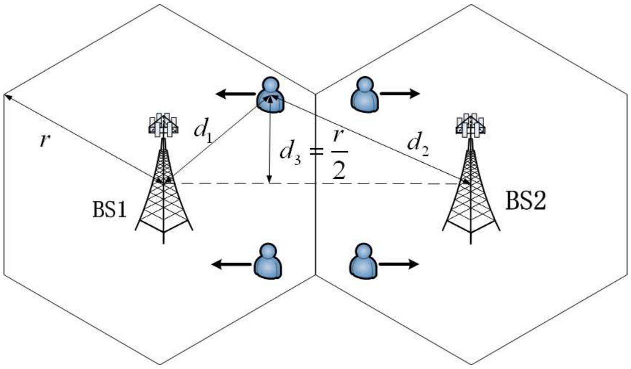

Fig. 3. MSs' positions in the simulated CoMP system. The locations of two MSs in the same cell are symmetrical to the line connecting the two BSs, and the MSs in different cells are symmetric to the cell edge. $d_3$ is fixed to be $\frac{r}{2}$. All MSs move from the cell edge to the cell center simultaneously, then their local receive SNRs all increase. Given the value of $d_1$, we can get the value of $d_2$ and vise versa. Assume that the downlink receive SNR of the cell edge MS, $\mathrm{SNR}_{edge}$, is 10dB. Consider the path loss factor $\epsilon$ as $3.76$, then the receive SNR of a MS from a BS with a distance $d$ can be computed as $\mathrm{SNR}(d) = \mathrm{SNR}_{edge} + \epsilon 10\log_{10}(\frac{r}{d})$. Similarly, when $\mathrm{SNR}(d)$ is given, we can get $d$.

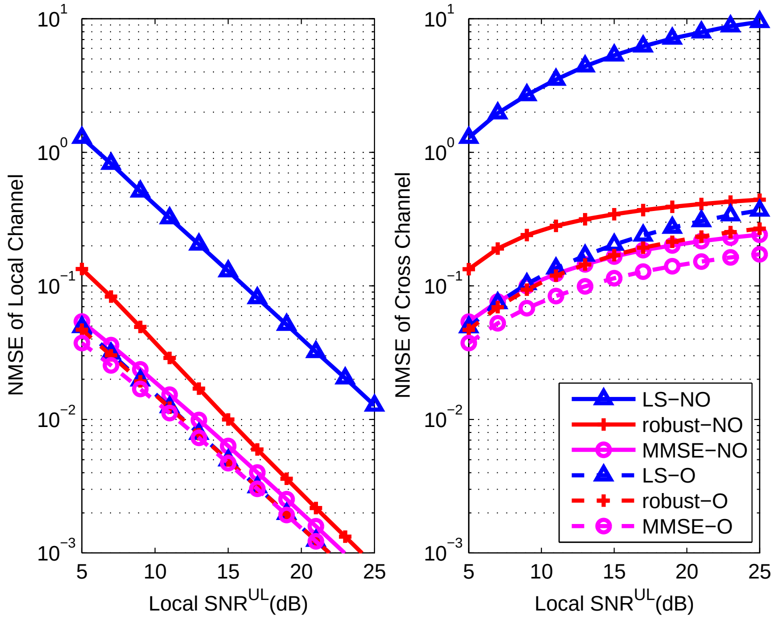

Fig. 4. NMSEs of different estimators for both local and cross channels versus the receive SNR of the local channel. The NMSEs are obtained by averaging over $1000$ realizations of small scale fading channels. The X-axis is defined as $\text{Local SNR}^{\text{UL}} = \frac{\alpha_{\text{local}}^2 p^u}{\sigma_n^2}$, where $\alpha_{\text{local}}^2$ is the large scale fading energy of the local channel for the MS. When the MSs are at the cell edge, $\text{Local SNR}^{\text{UL}} = 5$ dB. The Y-axis is the NMSE of channel estimators, which reflects the estimation performance of the small scale fading channels. When $\text{Local SNR}^{\text{UL}}$ increases, the large scale fading gains of the cross channels decrease, which leads to large NMSE of the cross channels. For the local channels, the NMSE of the three estimators are overlapped under orthogonal training (shown as "-O" in the legend). For the cross channels, the NMSE of the MMSE estimator under non-orthogonal training (shown as "-NO" in the legend) is overlapped with that of the robust estimator under orthogonal training.

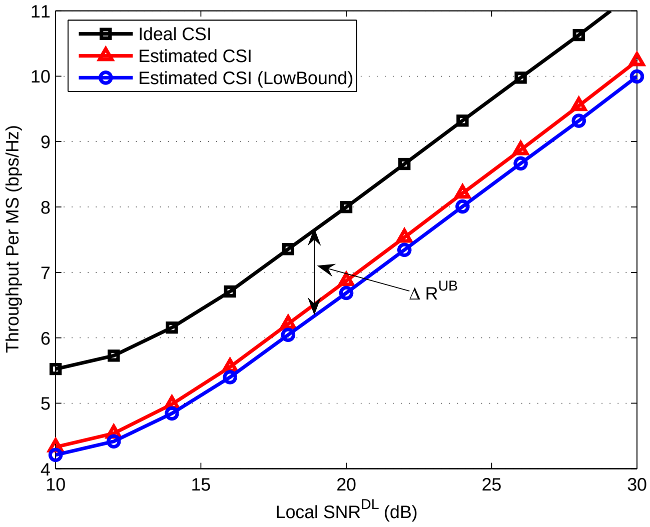

Fig. 5. Achievable rate and its lower bound of a MS when the MMSE estimator and orthogonal training are considered. The per MS rate of CoMP transmission with perfect CSI is also provided for reference, which is shown as "ideal CSI" in the legend.

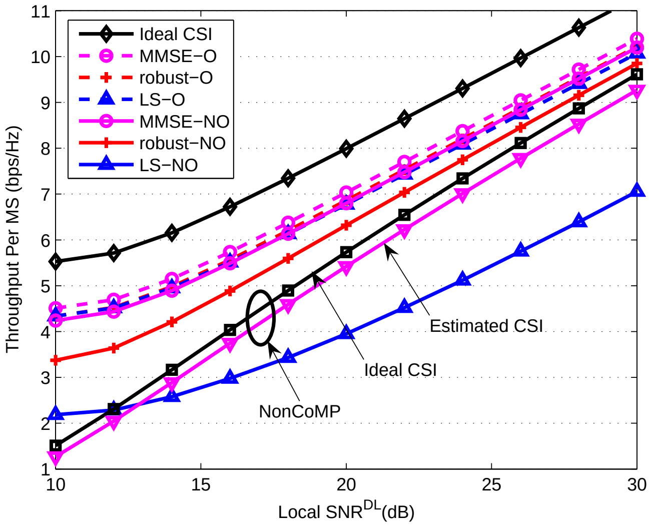

Fig. 6. Achievable rate of a MS when different estimators are used with both orthogonal and non-orthogonal training. For the Non-CoMP transmission with estimated CSI, the CSI for downlink precoding is estimated by the conventional single user MMSE estimator [8]. The performance when the robust estimator and the LS estimator under orthogonal training are applied overlap with that when MMSE estimator under non-orthogonal training are used. The meaning of the legends is the same as previous figures.

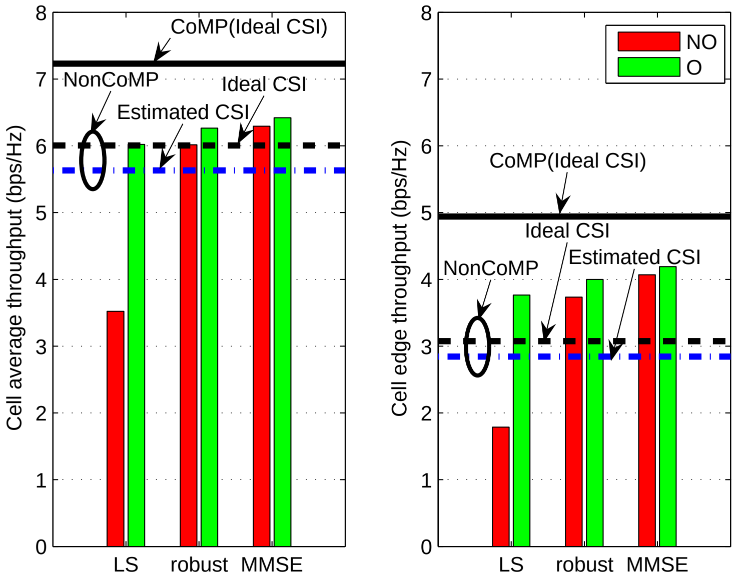

Fig. 7. Cell average and cell edge MS throughput when different channel estimators are used. The cell edge MS throughput is defined as the $5\%$ point of the cumulative distribution function of the MS throughput. As a baseline, the results of Non-CoMP transmission are also provided. The meaning of the legends is the same as previous figures.